SINTEF
PROCEEDINGS
4

Selected papers from the 10th Trondheim Conference on CO_2 Capture, Transport and Storage

TCCS-10

SINTEF Proceedings

Editors:
Nils A. Røkke and Hanna Knuutila

TCCS–10
CO_2 Capture, Transport and Storage
Trondheim 17th–19th June 2019

Selected papers

SINTEF Academic Press

SINTEF Proceedings no 4
Editors: Nils A. Røkke (SINTEF) and Hanna Knuutila (NTNU)
TCCS–10
CO_2 Capture, Transport and Storage. Trondheim 17th–19th June 2019
Selected papers from the 10th International Trondheim CCS Conference

Keywords:
CCS – Carbon Capture, Transport and Storage, CO_2 Capture, CO_2 Transport, CO_2 Storage, CO_2 Utilization, Pre-combustion capture, Post-combustion capture, Oxy-fuel capture, CCS and hydrogen, CO_2 positive solutions, International R&D activities, Whole system issues, Novel CCS technologies, Public Acceptance, Communication, Policy, Business models

Cover illustration: SINTEF Energy

ISSN 2387-4295 (online)
ISBN 978-82-536-1646-9 (pdf)

SINTEF Academic Press
Address: Børrestuveien 3
PO Box 124 Blindern
N-0314 OSLO
Tel: +47 40 00 51 00

www.sintef.no/community
www.sintefbok.no

SINTEF Proceedings
SINTEF Proceedings is a serial publication for peer-reviewed conference proceedings on a variety of scientific topics.
The processes of peer-reviewing of papers published in SINTEF Proceedings are administered by the conference organizers and proceedings editors. Detailed procedures will vary according to custom and practice in each scientific community.

EXPERIMENTAL STUDY OF THE USE OF PARTICLES FOR TRACKING THE INTERFACES IN PRIMARY CEMENTING OF CONCENTRIC AND ECCENTRIC WELLS

A. Taheri[1*], J.D. Ytrehus[2], A. Taghipour[2], B. Lund[2], A. Lavrov[2], M. Torsæter[2]

[1] NTNU, Trondheim, Norway

[2] SINTEF Industry, Trondheim, Norway

* Corresponding author e-mail: amir.taheri@ntnu.no

Abstract

In this study, our recent and new approach for detailed tracking of the interface between well fluid and cement by using particles is investigated. The particles can enable us to know the precise location of the interface between two fluids and be sure about displacement efficiency in the annulus. This includes the introduction of intermediate buoyant particles that reside at the interfaces between successive fluids in a well (e.g., cement-spacer or spacer-mud). Such particles must overcome strong secondary flows to travel with the interface. For this purpose, the displacement mechanisms of Newtonian and non-Newtonian fluids in the annulus of vertical and inclined wells is investigated by using an experimental set-up with concentric and eccentric annular geometries. For more efficient displacement, the displacing fluid should have a higher density than the displaced fluid, and the intermediate-buoyancy particles that reside at the interface between successive fluids are introduced into the models. Particle motions are investigated in models with different fluid rheology and displacement flow rates. This approach for tracking of the interface can improve the quality of annular cementing of CO_2 wells and thus the storage safety.

Keywords: *annular model, secondary flow, particle tracking*

1. Introduction

CO_2 capture and storage (CCS) is considered as one of the most promising solutions for decreasing the emissions of CO_2 into the atmosphere. Large-scale storage of CO_2 requires understanding the trapping mechanisms of CO_2 into storage sites to prevent and mitigate the leakages of CO_2 to the atmosphere. One part of the stored CO_2 in underground formations is free phase, and hence there is a chance of leakage of CO_2 out to the atmosphere. So the probable leakage points in the storage sites should be recognized. leak-free injection wells (or any other type of wells penetrating a CO_2 storage reservoir) are one of the main concerns in studies related to CO_2 leakage that enhance the demand for high-quality cement along the wellbore, between the casing and the rock formation. The main prerequisite for annular cement sheaths with high integrity and without any leakage paths is high efficiency in the displacement of the drilling fluid and the formation fluids from the annulus by sequential pumping of spacer and cement. For wells penetrating CO_2 storage reservoirs, it is especially important that all the annular cement columns are of high quality. This is because CO_2 is a buoyant fluid, and also such wells are subjected to harsh conditions (e.g., cooling of the well/formation, elevated pressure, and chemical reactions) [1].

One of the most critical operational factors that affect the quality of well cementing is the displacement of the drilling fluid and the formation fluids from the annulus by sequential pumping of spacer and cement. The procedure is such that non-Newtonian yield-stress fluids of progressively higher density and rheology are pumped into the well. Spacer is typically of higher density and rheology than drilling fluid, and cement is ideally of higher density and rheology than the other existing fluids in the annulus. This sequential pumping is done to stabilize the displacement process and the interfaces and to improve the displacement efficiency [2, 3]. Ideally, all the fluids in place are displaced evenly, and the cement takes their place without leaving any mud/spacer pockets or channels along the well. In reality, however, several factors prevent a perfect displacement. These include an uneven borehole due to soft rocks and washouts as well as the eccentric positioning of the casing within the borehole that is still very common, especially in inclined wellbores. Thus, fluid interfaces in the annulus typically do not advance uniformly along the well.

There are numerous computational studies of displacement flow in different geometries; annulus and unwrapped annulus or Hele-Shaw geometry [4, 5, 6 and 7]. There are few experimental studies about displacement flow in eccentric annular geometries. The first detailed study was performed by Tehrani et al. [8]. The experiments were performed in an inclined narrow annulus with an aspect ratio of 0.035 and a length of 3 m. They examined various flow rates and eccentricities, and the results were compared with modeling results in the form of final displacement efficiencies at the end of the experiments. They recorded both visualization data and conductivity changes in the set-up. They used non-Newtonian fluids and found reasonable qualitative agreement between experimental and modeling results. Experimental studies of the laminar flow of both Newtonian and non-Newtonian fluid displacements in vertical narrow eccentric annuli by Mohammadi et al. confirm that small eccentricity, increased viscosity ratio,

increased density ratio, and slower flow rates appear to favor a steady displacement for Newtonian fluids. They believed that qualitatively the same results could be achieved for non-Newtonian fluids, while the role of flow rate is less clear. The secondary flow and dispersion had a dominant effect on the results [9]. In an eccentric annulus where a displacing fluid tends to pass through the wide side, a positive density difference between two fluids produces a hydrostatic pressure imbalance between the wide and narrow sides. This imbalance causes a secondary azimuthal current on the main axial flow whose direction is from the wide side to the narrow side of the annulus in the displacing fluid and from the narrow side to the wide side in the displaced fluid [10].

Since there is no direct access to well annuli, operators have to rely on indirect methods when evaluating the quality of a cementing job. Cement bond log (CBL) is the most popular tool in this case where the degree of zonal isolation is inferred from the degree of acoustic coupling of the cement to the casing and formation. The log can reveal large channels in cement but is not very sensitive to minor channels (de-bonding and micro-annuli). Moreover, the logging is done after finishing the cement job and when the cement has hardened. This means that there is no room left for corrective measures if the cement job went wrong, except performing remedial cementing which requires perforating the casing. Temperature logs, which sense the exothermic cement hardening, can also be performed after placement to detect the top of annular cement. Such logs can, however, not be used to evaluate the quality of the cement column, e.g., the presence of voids or mud pockets. In the past, radioactive tracers were injected together with cement to determine the top of the annular cement column, but this method was abandoned due to HSE issues.

The primary objective of this study is to introduce and check a new approach for more accurate and detailed tracking of the interface between mud and cement by using particles. The particles can enable us to know the precise location of the interface between two fluids and be sure about displacement efficiency in the annulus. This includes the introduction of intermediately buoyant particles that reside at the interfaces between successive fluids in a well (e.g., cement-spacer or spacer-mud). The tracing can happen using radioactive or electromagnetic tracer devices. This use of particles for tracking the interface between fluids in annular displacement flow was studied previously by Frigaard and Maleki by solving the Hele-Shaw model equations and placing the particles in the model. The important active forces in this situation are the drag force and gravity force corrected by the effect of buoyancy. The difference between the wide/narrow side far-field velocity and the mean velocity is a measure of the secondary flow near the interface. Such particles must overcome strong secondary flows in order to travel with the interface. Frigaard and Maleki introduced a dimensionless number by involving fluids and particles properties ($Bu = [(\rho_2 - \rho_1)gd_p^2]/\mu\bar{w}$) and defined a minimum value of 18 for this number for particle selection to be sure that the particles can reach and travel with the interface. In this equation, d_p is the particle diameter, μ is the fluid viscosity, $\bar{w}$ is the mean speed of the interface between two fluids that advance steadily along the annulus, and ρ_1 and ρ_2 are densities of displaced and displacing fluids [11 and 12].

This study consists of two sections. After describing the experimental set-up and the used fluids in the experiments, the results of several flow displacement tests are described. The main purpose of this section is to study the behavior of the interface between two fluids in the flow displacement tests with different pairs of Newtonian/non-Newtonian fluids and different flow rates. In the next section, results of the additional flow displacement tests are reviewed where particles are released at the interface between two fluids, and the goal of this section is to study the behavior and motion of the particles in between of the two fluids during displacement flow with different specified flow rates.

2. Experimental Description

2.1 Experimental Set-up and procedure

A picture of the annular experimental set-up is shown in Figure 1. The experimental tests were performed in a 110 cm long transparent plexiglass tubing with an aluminum tubing (plexiglass tubing in the concentric model) as the inner body. The inner radius of the outer tubing (r_o) and the outer radius of the inner tubing (r_i) are 5.5 and 3.5 cm, respectively. The aspect ratio of circumferential and radial length scales (δ) is defined by $\delta = (r_o - r_i)/\pi(r_o + r_I)$ that is 0.071 in this geometry. The field range for δ is typically in the range of 0.01-0.1 [9]. The scaled length of the model is 7.78 by considering the length scale (L) of 14.14 cm ($L = 0.5\pi(r_o + r_i)$). The distance between the centers of the inner and outer tubings (d) in the eccentric models is 8 mm that corresponds to an eccentricity of 0.4. Our experiments were conducted at two inclinations; $\Theta = 0^o$ (vertical) and $\Theta = 10^o$ (inclined toward the narrow side).

The flow rate during the tests is controlled. Two pumps are required for the flow of displacing and displaced fluids. A centrifugal pump is used for the displacement of the displaced fluid. For the displacing fluid, we use a centrifugal pump as well, and a variable frequency drive controls the flow rate. A Heinriches magnetic flow meter with the output signal of 4-20 mA corresponding to 0-150 l/min is used to measure the flow rate. Moreover, eight conductivity probes have been installed at the two levels of the model for tracking the conductivity of the fluids in contact. Our previous studies show that there is not any consistency between our qualitative visualization in the flow displacement tests and the recorded conductivity changes by the probes and a plausible explanation was that displaced fluids bonds to the probes, and it prevents contact between the probes and the conductive displacing fluid. [13]. So we will not consider the readings by the conductivity probes in this study.

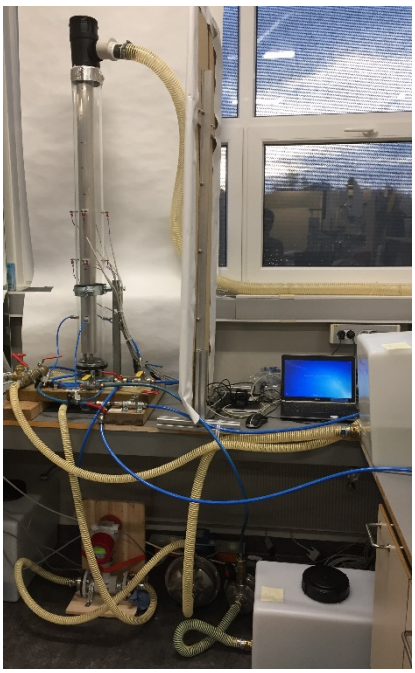

Figure 1: The Experimental Annular Set-Up

For performing the tests and at the beginning, the annulus is filled by a displaced fluid, and this fluid is displaced by a displacing fluid from the bottom and with a specified flow rate. In the cases with particles, the initial displaced fluid is displaced by the displacing fluid with a very small flow rate in order to have a flat interface between the two fluids around 0.2 m above the bottom of the model. Afterward, the particles are released below the interface from four particle ports, and the displacing fluid with the specified flow rate displaces the displaced fluid from the bottom. We used Fluorescent Red Polyethylene Microspheres from Cospheric with diameters of 27-32um and 425-500um and a density of 1.090 g/cc in the tests. Images of the displacement process are recorded using a Canon EOS 5D Mark IV camera at one-second intervals.

2.2 Fluid Preparation and Analysis

In these series of experiments, several pairs of Newtonian and non-Newtonian fluids are prepared and used. Water and sucrose solution are the used Newtonian fluids, and Carbopol-980 solution with different concentrations are the used non-Newtonian fluid with shear thinning and yield stress behavior. Carbopol is widely used as a thickener, stabilizer, and suspending agent. The rheology of Carbopol is significantly influenced by the concentration and pH of the solution, and the yield stress is developed at an intermediate pH on neutralizing with a base agent (in our case NaOH). The neutralized solution is fairly transparent and has the same density as water (for low concentrations). In preparing the Carbopol-980 solution, we gradually add the Carbopol powder (0.1-0.15 wt/wt%) to water in a mixing tank. Mixing proceeds slowly for a few hours. Since the Carbopol concentration in our experiments is not very high, 3-4 hours of mixing is enough. When adding NaOH to the Carbopol–water solution, we have to decrease the mixing rate and be careful not to introduce air bubbles into the gel-like solution. Brilliant Cresyl Blue, a cationic dye that is stable and water-soluble, is added to the displaced fluids for visualization purposes [14]. Rheological measurements showed that this dye does not affect the rheology of the fluids. NaCl is also added to the displacing fluid to be able to measure the fluid conductivities.

Fluid densities and pHs were measured using a DMA-46 densitometer (Anton Paar) and pH meter pH 1000 L (VWR International) respectively. Rheology of fluids was tested before each experiment using Anton Paar MCR 102 rheometer. The temperature was fixed at 21°C. The Carbopol-980 solution rheology data were fitted to a Herschel-Bulkley model $\tau = \tau_y + k\dot{\gamma}^n$ where τ_y is yield stress, κ is consistency index, and n is a power-law index. In order to reset the structure of the polymers between samples, all rheology tests were subjected to a pre-shear of 2 min with a shear rate of 1100 s^{-1} in the rheometer before data acquisition. After pre-shearing, the stress values were recorded by the rheometer for a decreasing and increasing ramp of shear rates (to check for possible hysteresis) in a logarithmic manner.

Table 1 presents an overview of the performed tests, and Table 2 shows the properties of the used fluids in the tests. Subscripts 1 and 2 are representative of displaced and displacing fluids, respectively. Figure 2 compares the rheology behavior of three different non-Newtonian fluids in the tests no. 8 and 11 in a log-log coordinate. From this figure, it can be seen that the yield stress of the displaced fluid in the test no. 8 is higher than the yield stress of the fluids in the test no. 11 and displaced and displacing fluids in the test no. 6 have almost the same rheology. Figure 3 shows the effective viscosities of these fluids and it can be seen that at the range of displacement flow rates (shear rates more than 1 s^{-1}), the viscosity of the displacing fluid in the test no. 11 is more than the viscosity of the displaced fluid in this test, and the viscosity of the displaced fluid in the test no. 8 is less than the other viscosities in this comparison while its yield stress is more than the yield stress of the other ones.

Table 1: The Description of the Performed Tests

Test	Model Type	Displaced Fluid	Displacing Fluid	Model Inclination (degree)	Displacement Flow Rate (L/min)	Particle Size (um)
1	Concentric	Water	Sucrose Solution	0	6.33	500
2	Eccentric	Water	Sucrose Solution	0	10.09	-----
3	Eccentric	Water	Sucrose Solution	0	9.98	425-500
4	Eccentric	Water	Sucrose Solution	0	16.29	425-500
5	Eccentric	Water	Sucrose Solution	10	15.05	425-500
6	Eccentric	Water	Sucrose Solution	0	14.74	27-32
7	Eccentric	Carbopol Solution	Sucrose Solution	0	12.81	425-500
8	Eccentric	Carbopol Solution	Sucrose Solution	10	17.21	425-500
9	Eccentric	Carbopol Solution	Carbopol Solution	0	7.93	-----
10	Eccentric	Carbopol Solution	Carbopol Solution	10	7.47	-----
11	Eccentric	Carbopol Solution	Carbopol Solution	0	4.36	-----
12	Eccentric	Carbopol Solution	Sucrose Solution	10	16.6	-----

Table 2: Properties of the Fluids Used in the Tests at 21° C

Test	ρ_1 (g/cm3)	τ_{y1} (Pa)	κ_1 (Pa s^n)	n_1	ρ_2 (g/cm3)	τ_{y2} (Pa)	κ_2 (Pa s^n)	n_2
1	0.9950	0	0.000956	1	1.1274	0	0.002829	1
2	0.9950	0	0.000956	1	1.1274	0	0.002829	1
3	0.9950	0	0.000956	1	1.1274	0	0.002829	1
4	0.9950	0	0.000956	1	1.1274	0	0.002829	1
5	0.9950	0	0.000956	1	1.1274	0	0.002829	1
6	0.9950	0	0.000956	1	1.1274	0	0.002829	1
7	0.9996	0.92	2.90	0.44	1.1274	0	0.002829	1
8	0.9990	1.77	2.69	0.44	1.1243	0	0.002878	1
9	0.9990	1.13	4.22	0.42	0.9990	0.4	2.66	0.46
10	0.9990	1.13	4.22	0.42	0.9990	0.4	2.66	0.46
11	0.9990	0.45	3.52	0.59	0.9992	0.35	4.37	0.66
12	0.9990	0.92	2.90	0.44	1.1243	0	0.002878	1

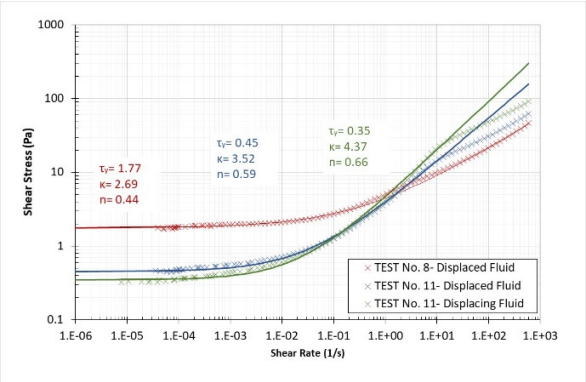

Figure 2: Rheological Behavior of the Carbopol-980 Solutions

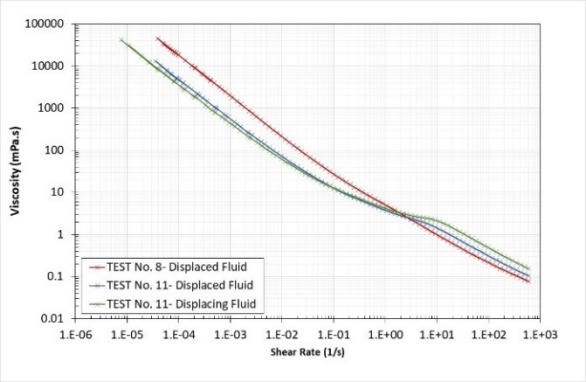

Figure 3: Viscosity of the Carbopol-980 Solutions

3. Experimental Results and Discussion

3.1 Displacement Flow Tests

In this section, the results of several displacement flow tests in the eccentric models are described. The tests were performed using different pairs of Newtonian and non-Newtonian fluids with different displacement flow rates mentioned in Table 1.

Figure 4 shows the snapshots of displacement flow in the test no. 2, where one Newtonian fluid is displaced with another one with higher viscosity and density and with a displacement flow rate of 10.09 L/min. From time 0 s that is the start of the displacement till time 36 s that is the end of displacement, it can be seen that there is a uniform and piston-like displacement in this test. While the displacing fluid tends to pass through the wide side (right-hand side), strong secondary flow from wide side to the narrow side in the displacing fluid causes piston-like displacement and a flat interface between the two fluids. In fact, secondary flow helps for more efficient and piston-like displacement in this case. Figures 5 and 6 represent snapshots of displacement flows in tests no. 9 and 10 where a non-Newtonian fluid with a lower viscosity displaces another non-Newtonian fluid with a higher viscosity and the same density. Model inclinations in the tests no. 9 and 10 are 0 and 10 degrees respectively, and the displacement flow rates in both cases are almost the same (7.93 L/min and 7.47 L/min in test no. 9 and 10 respectively). In both cases, a non-stable displacement is achieved, and the interface between the two fluids is not piston-like. While the displacing fluid advances toward the wide side of the annulus and reaches to the top of the model within 21 s, displaced fluid in the narrow side does not move. This can be due to a weak secondary flow in the model because of the high viscosity of the fluids and also viscous fingering due to the unstable displacement and displacing of a higher viscous fluid with a lower viscous fluid. Figure 7 shows the snapshots of displacement flow in the test no. 11 where both displaced and displacing fluids have almost the same viscosities (refer to Figure 3) and densities. While the yield stress of the displaced fluid (0.45 Pa) is higher than the yield stress of the displacing fluid (0.35 Pa), other rheological parameters cause the viscosity of the displacing fluid to become a bit higher than the viscosity of the displaced fluid in the range of the flow rate in the test. Also, the small flow rate of 4.36 L/min in the test decreases the chance of viscous fingering. Again, we see significant displacement from the wide side and a little movement of displaced fluid from the narrow side. The weak secondary flow in this test is the main reason for the un-stable displacement and the non-flat interface. Figure 8 shows the snapshots of displacement flow in the test no. 12, where a non-Newtonian fluid is displaced with a Newtonian fluid with higher density and lower viscosity. The displacement flow rate is 16.6 L/min and again we can see from the snapshots that due to a weak secondary flow (because of high viscosity in the displaced fluid) and probably viscous fingering (due to high flow rate and displacing of a high viscous fluid with low viscous fluid), the displacement is not stable and the interface between the two fluids is not flat.

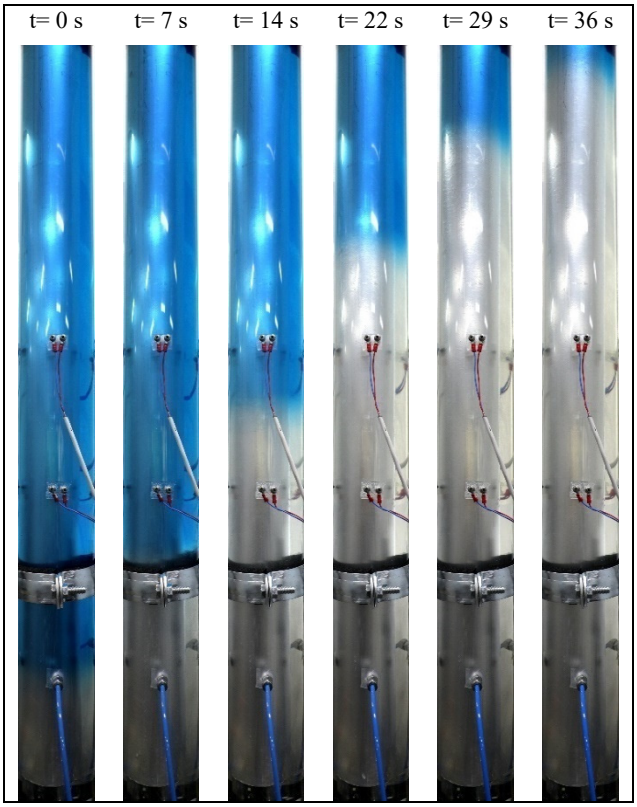

Figure 4: Snapshots of Displacement Flow in Test no. 2

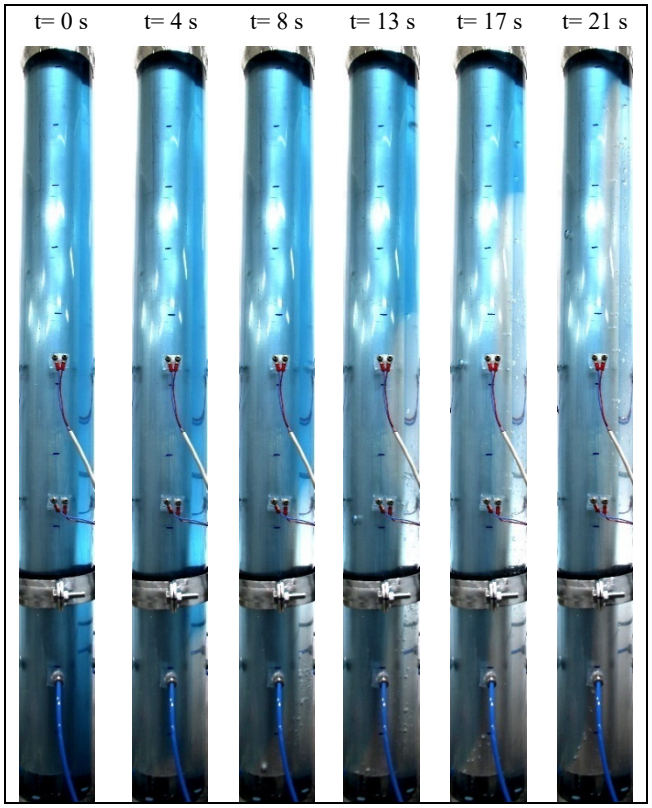

Figure 5: Snapshots of Displacement Flow in Test no. 9

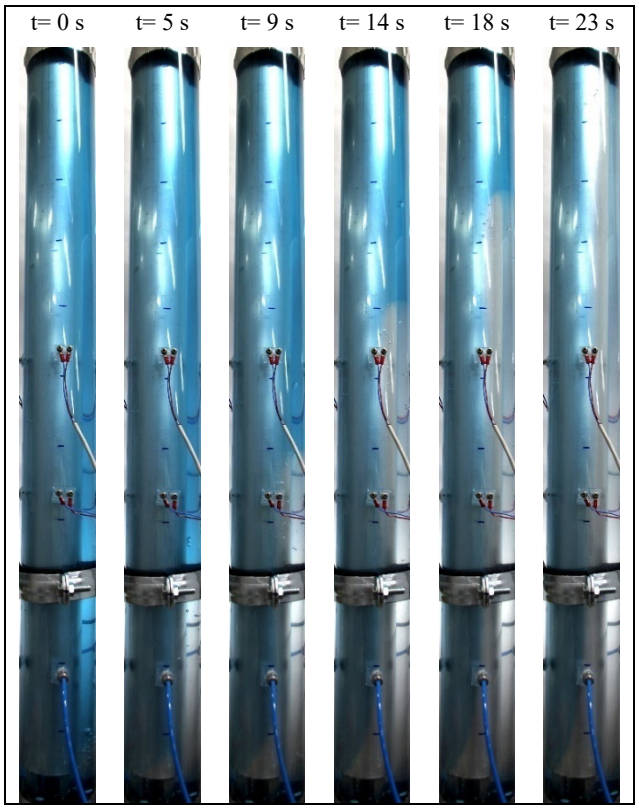

Figure 6: Snapshots of Displacement Flow in Test no. 10

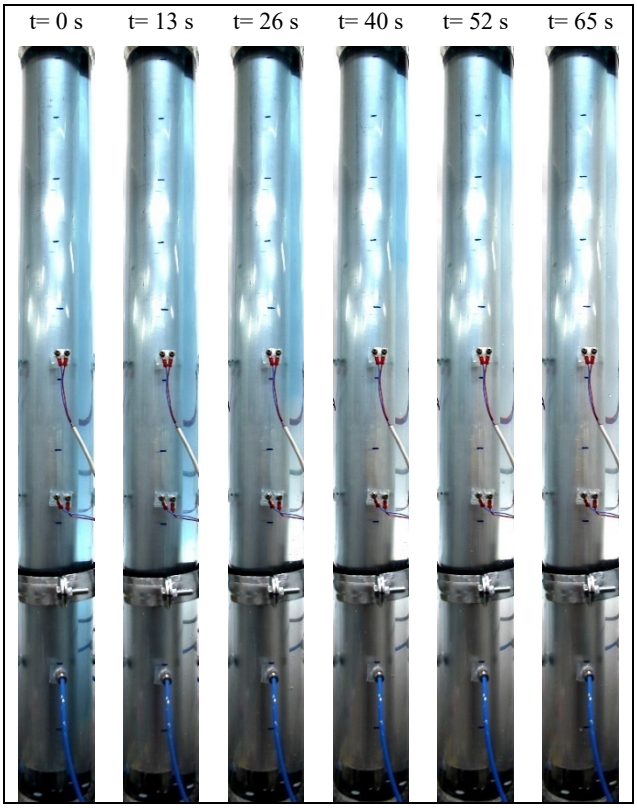

Figure 7: Snapshots of Displacement Flow in Test no. 11

Figure 8: Snapshots of Displacement Flow in Test no. 12

3.2 Particle Behaviors in Displacement Flow Tests

In these sets of the tests, the main objective is the study of the behavior and motions of particles for tracking of the interface in the models with different pairs of fluids. In each test, a fixed amount of particles is released from each four particle ports on the wall of the annulus and below the interface between the displaced and displacing fluids. After a few minutes, the particles distribute uniformly below the surface, and we observe uniform dispersion of the particles from the narrow side to the wide side of the annulus at the time of 0 s. Then the flow starts with a specified value, and the behavior of these particles on the interface of the displaced and displacing fluids is observed.

3.2.1. Concentric Model

Figure 9 shows the snapshots of displacement flow in the vertical concentric model in the test no. 1 where a Newtonian fluid with a higher viscosity and density displaces another Newtonian fluid with lower density and viscosity with a displacement flow rate of 6.33 L/min. This displacement scheme causes no viscous fingering that is obvious in the snapshots also. So due to the lack of eccentricity and viscous fingering we can see piston-like and stable displacement. The released particles with a diameter of 425-500 um also follow the interface and it can be seen that the particles have the capability of tracking the interface in the lack of existence of secondary flow in this concentric model.

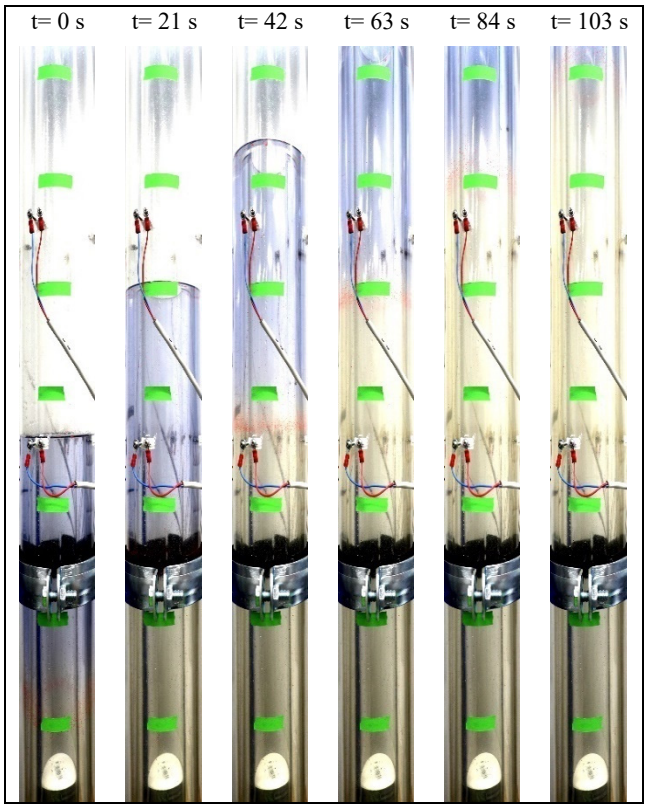

Figure 9: Snapshots of Displacement Flow in Test no. 1

3.2.2. Eccentric Models

Figure 10 shows snapshots of flow displacement by two Newtonian fluids in a vertical model in the test no. 3 from the start till the end of the process at the time of 31 s. It can be seen after the start of the flow with a flow rate of 9.98 L/min, the interface between the two fluids is almost flat, and we can see a piston-like displacement flow. Displacement flow is stable because the displacing fluid has higher density and viscosity than the displaced fluid, and there is no occurrence of viscous fingering. Moreover, the uniform piston-like displacement in this eccentric model confirms the high effect of secondary flow from the wide side to the narrow side in the displacing fluid and from the narrow side to the wide side in the displaced fluid. If we look at the motions of the red particles with a diameter of 425-500 um in the annulus, it is observed that after the start of the flow the particles move from the narrow side to the wide side and accumulate below the interface at the wide side. In fact, the secondary flow affects the particles and causes movement of particles from the narrow side to the wide side. Figure 11 shows the snapshots of flow displacement in the test no. 4 with the same fluids of the test no. 3. The only difference is the displacement flow rate that is higher in the test no. 4 (16.29 L/min) than the test no. 3. The same results are concluded from this test with a higher displacement flow rate. The interface between the two fluids is almost stable, and the piston-like displacement flow confirms the existence and high effect of secondary flow. This secondary flow has an effect on the released red particles in the model, and they move from the narrow side to the wide side and accumulate below the interface at the wide side and move upward by the interface.

Figure 12 shows the snapshots of displacement flow in the test no. 5 in an eccentric model that is inclined 10^{o} to the narrow side. The used displaced and displacing fluids are the same as the previous tests, and the flow rate is 15.05 L/min. In these snapshots, a stable piston-like displacement with a flat interface with a 10^{o} dip is observed. When we look at the motions of the red particles, we can see a difference compared to the first two tests. It can be observed that the uniformly dispersed particles with a diameter of 425-500 um below the interface move by the interface, indicating that they overcome the strong secondary flow. In this test, the particles track the interface accurately.

Figure 13 presents snapshots of the displacement flow in the test no. 6 in a vertical model and with Newtonian fluids like before. Again, we can see stable and piston-like displacement in this test. The released particle in this test have a diameter of 27-32 um, and the particles are not observable in the captured images by eye. However, they affect the blue color of the displaced fluid and change the blue color to purple-blue color. By looking into the snapshots from the start till the end of this test, it can be seen that the fluid color around he interface is purple-blue and it can be stated that these particles are able to track the interface and the strong secondary flow around the interface has no effect on them.

Figure 14 shows the snapshots of displacement flow in the test no. 7 in the same model by using the same

displacing fluid and one non-Newtonian fluid and flow rate of 12.81 L/min. In this case, it is observed that secondary flow has not any significant effect on displacement efficiency due to the higher viscosity of the displaced fluid, and the interface between the two fluids is not piston-like. By looking into these snapshots at different times, it is observed that almost all the red particles with a diameter of 425-500 um move from the narrow side to the wide side and move by the interface toward the top of the model. Figure 15 presents the snapshots of the displacement flow in the test no. 8 using the same Newtonian displacing fluid and a non-Newtonian displaced fluid with higher yield stress than the displaced fluid in the test no. 7. The displacement flow rate is 17.21 L/min that is more than the previous tests. From these snapshots, it can be seen that there is no uniform and stable displacement in this test due to the very weak secondary flow around the interface. Moreover, the displacing fluid had lower viscosity and higher density than the displaced fluid that cannot guarantee a stable displacement. Also, the high flow rate increases the chance of viscous fingering. All of these phenomena cause non-piston like displacement. Also, the high yield stress of the displaced fluid and lower viscosity of the displacing fluid causes bypassing of the displaced fluid by the displacing fluid. The released particles with a diameter of 425-500 um are under different forces, and they do not follow the interface in this test.

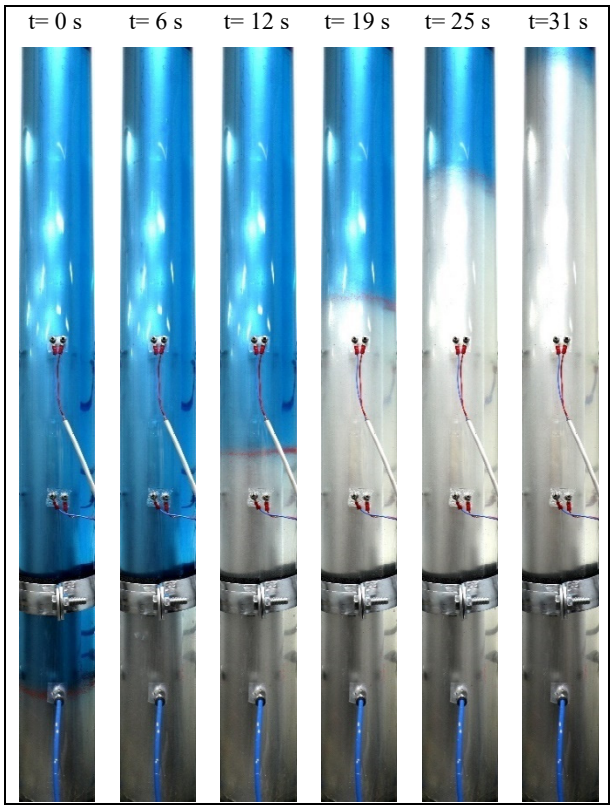

Figure 10: Snapshots of Displacement Flow in Test no. 3

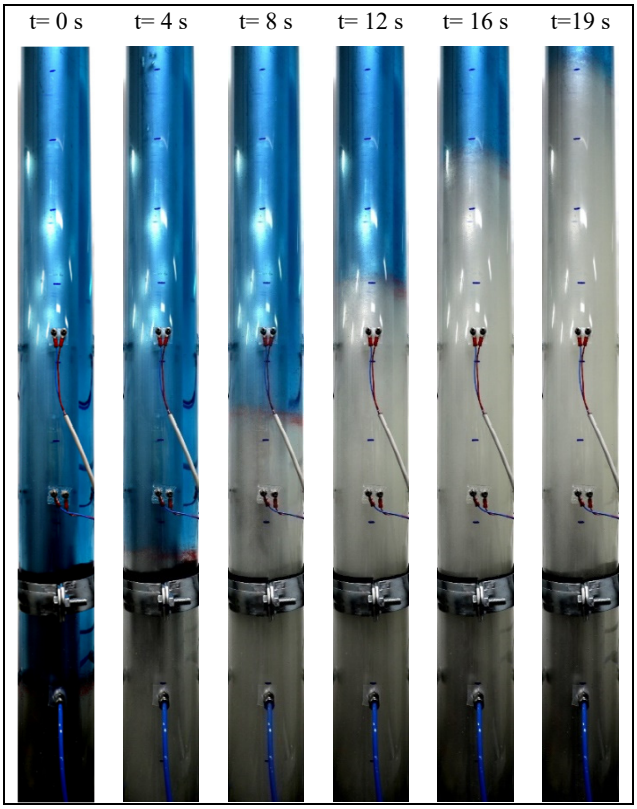

Figure 11: Snapshots of Displacement Flow in Test no. 4

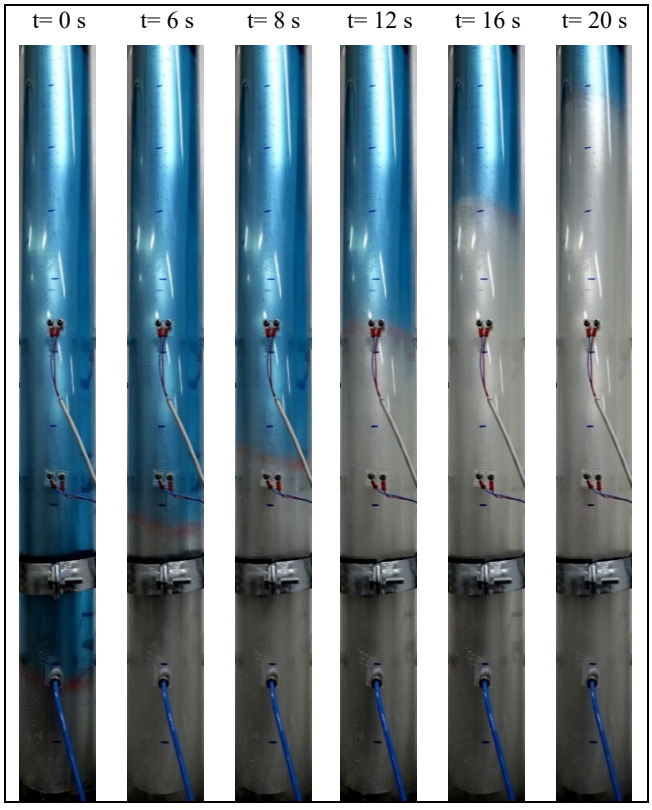

Figure 12: Snapshots of Displacement Flow in Test no. 5

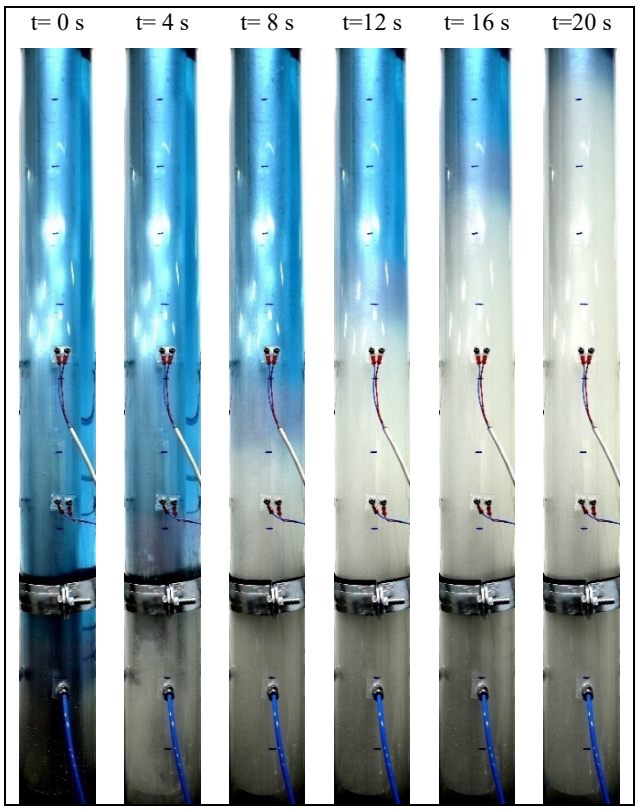

Figure 13: Snapshots of Displacement Flow in the Test no. 6

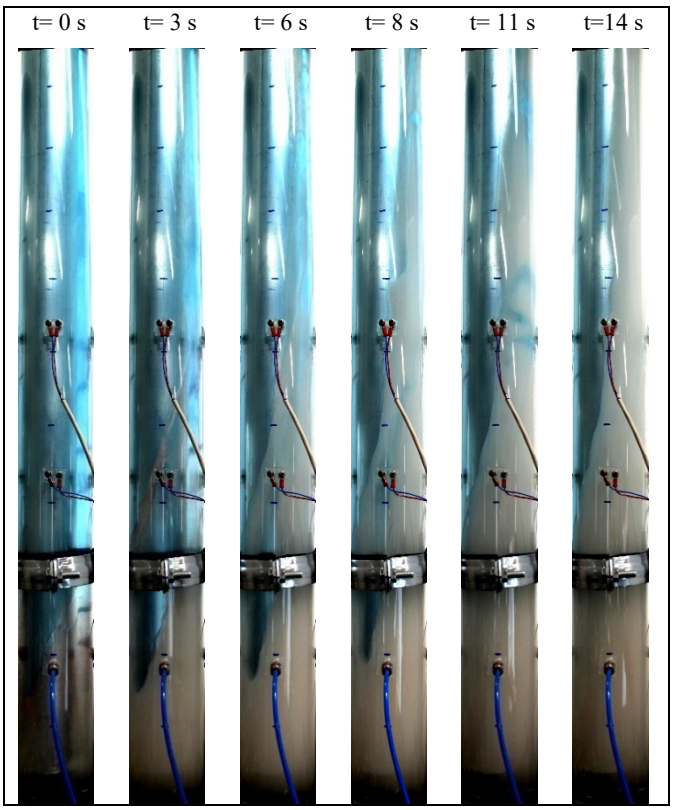

Figure 15: Snapshots of Displacement Flow in Test no. 8

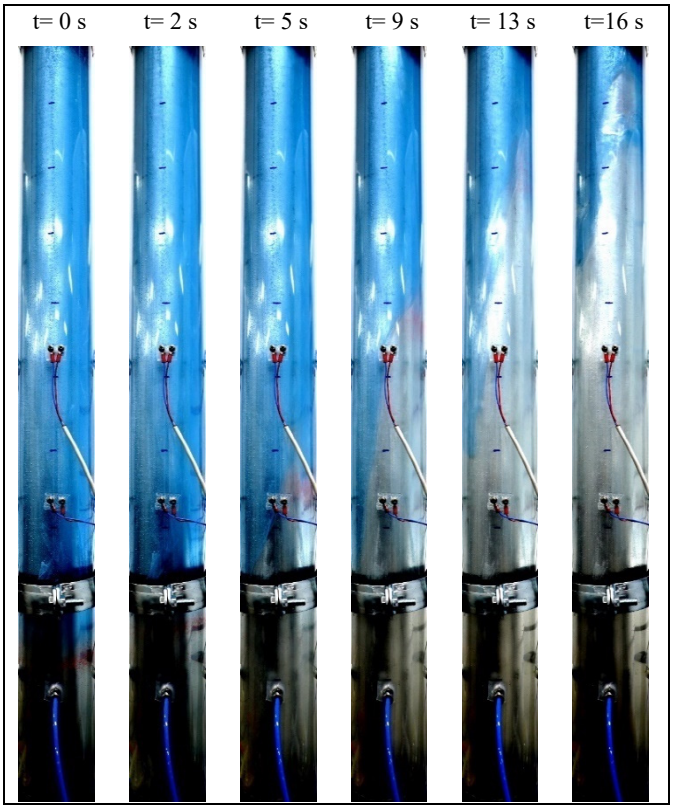

Figure 14: Snapshots of Displacement Flow in Test no. 7

Conclusions

Drag force and gravity force corrected by the effect of buoyancy are the active forces in particle motions in the tracking of the interface between two fluids in displacement flows. The experimentally performed annulus displacement flow in the concentric and eccentric models using Newtonian and non-Newtonian fluids confirm that:

1- Viscous fingering and secondary flow are two crucial displacement mechanisms that affect the efficiency and stability of displacement in annulus models.

2- Particles with a diameter range of 425-500 um are able to track the interface between fluids in the concentric model.

3- Particles with a diameter range of 425-500 um are not able to overcome strong secondary flows in the vertical eccentric models and particles move from the narrow side to the wide side and travel upward by the interface. In the models with a small inclination to the narrow side and when the displacing and displaced fluids have Newtonian behavior, the released particle below the interface resides on the interface, and they can track the interface until the end of the process appropriately.

4- Particle with a diameter range of 27-32 um has enough potential to overcome the secondary flow in a model where both displacing and displaced fluids have Newtonian behavior and the displacement is stable and the interface is flat.

Acknowledgments

This publication has been produced in the project "Studying moving fluid interfaces during cementing of CCS wells" funded by the Research Council of Norway (268510/E20).

References

[1] Lavrov, A., and Torsæter, M., 2016, "Physics and Mechanics of Primary Well Cementing", Springer.

[2] Bishop, M., et al., 2008, "A robust, field friendly, cement spacer system", AADE-08-DF-HO-07 paper presented at the 2008 AADE Fluids Conference and Exhibition held at the Wyndam Greenspoint Hotel, Houston, Texas, April 8-9. 2008.

[3] Nelson, E.B. and D. Guillot, 2006, "Well cementing", Schlumberger.

[4] Bittleston, S., Ferguson, J., and Frigaard, I. A., 2002, "Mud removal and cement placement during primary cementing of an oil well- Laminar non-Newtonian displacements in an eccentric annular Hele-Shaw cell", J. Eng. Math., 43, pp. 229–253.

[5] Pelipenko, S., and Frigaard, I. A., 2004, "On steady state displacements in primary cementing of an oil well", J. Eng. Math., 46, pp. 1–26.

[6] Pelipenko, S., and Frigaard, I. A., 2004, "Two-dimensional computational simulation of eccentric annular cementing displacements", IMA J. Appl. Math. 69, 557–583.

[7] Pelipenko, S., and Frigaard, I. A., 2004, "Visco-plastic fluid displacements in near-vertical narrow eccentric annuli: prediction of travelling-wave solutions and interfacial instability", J. Fluid Mech., 520, pp. 343–377.

[8] Tehrani, A., Ferguson, J., and Bittleston, S., 1992, "Laminar displacement in annuli: A combined experimental and theoretical study", In Society of Petroleum Engineers.

[9] Mohammadi, S. M., Carrasco-Teja, M., Storey, S., Frigaard, I. A., and Martinez, D. M., 2010, "An experimental study of laminar displacement flows in narrow vertical eccentric annuli", J. Fluid Mech. 649, 371.

[10] Tehrani, A., Bittleston, S. H., and Long, P.J.G., "Flow instabilities during annular displacement of one non-Newtonian fluid by another", Experiments in Fluids, 14 (1993), pp. 246-256.

[11] Maleki, A., and Frigaard, I. A. , 2018, "Tracking fluid interfaces in primary cementing of surface casing", Physics of Fluids 30, 093104.

[12] Frigaard, I. A., and Maleki, A., 2018, "Tracking Fluid Interface in Carbon Capture and Storage Cement Placement Application", Paper No. OMAE2018-77630, pp. V008T11A060.

[13] Taheri, A., Ytrehus, J.D., Taghipour, A., Lund, B., Lavrov, A., and Torsæter, M., 2019, "USE of tracer particles for Tracking fluid interfaces in primary cementing", OMAE paper no. 2019-96400, presented at the 38th International Conference on Ocean, Offshore and Arctic Engineering (OMAE2019), June 9-14, 2019, Glasgow, Scotland.

[14] Qwabe, L., Pare, B., and Jonnalagadda, S. B., 2005, "Mechanism of Oxidation of Brilliant Cresyl Blue with Acidic Chlorite and Hypochlorous Acid. A Kinetic Approach", S. Afr. J. Chem., 58, 86–92.